RCS Enhancement of Millimeter-Wave LTCC Van Atta Arrays With 3-D Printed Lenses for Chipless RFID Applications

Kamil Trzebiatowski, Weronika Kalista, Lukasz Kulas, *Senior Member, IEEE*, and Krzysztof Nyka, *Senior Member, IEEE*

***Abstract*—In this letter, we present a new method to enhance the radar cross section (RCS) of Van Atta arrays, which can be used in chipless radio frequency identification tags operating in millimeter-wave frequency bands. Small planar low-temperature co-fired ceramic (LTCC) Van Atta arrays, which are durable and can operate in harsh environments, are combined with 3-D printed lenses to increase or modify the shape of their RCS by up to 10 dB. The lenses are uniform in one direction to maintain a wide RCS angular range of the underlying Van Atta arrays. They are manufactured using an affordable 3-D printing stereolithography process using high-performance resin. The resulting manufactured and measured Van Atta retrodirective arrays integrated with lenses exhibit measured RCS levels up to −28 dBsm at 24 GHz frequency. Moreover, the proposed approach allows LTCC Van Atta tags to be easily modified and reused by exchanging their lenses to adapt them to a new application. To the best of the authors' knowledge, this is the first time an experimental evaluation of lenses combined with Van Atta arrays has been presented. This novel technique can also be integrated with other RCS enhancement methods to further increase RCS levels.**

***Index Terms*—3-D printing, additive manufacturing, chipless radio frequency identification, circular economy, lenses, millimeter-wave (mmW) antenna, retrodirective arrays, sustainability, Van Atta arrays.**

I. Introduction

THE chipless radio frequency identification (RFID) systems are getting more attention as a low-cost and energy efficient alternative to conventional RFID systems [1], [2], [3], [4]. Unlike traditional tags, chipless RFID tags lack integrated circuits, significantly reducing their manufacturing costs. Various designs of such tags have been proposed in the literature, such as resonator- or delay-line-based tags [1], [2], [3], [4], [5], [6], [7]. Chipless RFID systems are being developed especially in millimeter-wave (mmW) bands because integrated circuits for these bands are either unavailable or very expensive [1], [2], [3]. The use of mmW bands theoretically offers better angular resolution and improved spatial discrimination of tags due to the narrow beams of the antenna, allowing for more precise identification and tracking of items in densely packed environments.

The main challenges associated with RFID tags are their relatively short interrogation range, typically measured in centimeters [8], and the requirement for precise alignment between the reader and the tag [3], [8]. This limitation is especially pronounced in mmW bands, where the effective aperture of the antennas is small, leading to low radar cross section (RCS) levels. To overcome the short-range problem, RFID tags with increased RCS levels should be employed. One possible approach is to replace single radiators with high-gain antenna arrays having a large effective aperture. However, higher directivity of such an array inevitably results in a narrower beam and smaller angular interrogation range, making it challenging to read the tags from various angles [9].

Van Atta arrays [10], [11] offer a solution to the above problem by exhibiting retrodirective properties, meaning they reradiate incident waves back to the source over a wide range of angles. This retrodirective behavior is achieved by appropriately arranging and interconnecting the transmitting and receiving radiating elements in the array [10], [11], [12]. The elements in a Van Atta array can be interconnected with symmetry along a single axis (1-D arrays) or along both axes (2-D arrays). In the 1-D array, there is just one retrodirective plane (the main plane), in which it reflects the signal back to the source in a wide range of angles, while along the perpendicular plane the array inherits the properties of separate array elements. In the 2-D array, both planes exhibit retrodirective behavior.

Unlike for an ordinary scatterer, the equivalent RCS of a retrodirective array is directly related to the total gain of the array instead of its physical cross section [11]. Thus, Van Atta arrays with high RCS levels can be created by increasing the

Received 9 September 2024; revised 10 October 2024; accepted 1 November 2024. Date of publication 6 November 2024; date of current version 5 February 2025. This work was supported in part by the M-ERA.NET 3 Partnership for research and innovation on materials and battery technologies, European Union's Horizon 2020 research and innovation programme, Germany (Sächsisches Staatsministerium für Wissenschaft, Kultur und Tourismus (SMWK)), and Poland (National Centre for Research and Development (NCBiR)), through LDI MAGIC project under Grant project9280; in part by the European Union and Chips Joint Undertaking and its members (The Netherlands, Austria, Germany, Spain, Finland, France, Latvia, Poland and Sweden) through the SUSTRONICS project under Grant 101112109; and in part by the Swiss State Secretariat for Education, Research and Innovation (SERI). *(Corresponding author: Kamil Trzebiatowski.)*

Kamil Trzebiatowski, Weronika Kalista, and Krzysztof Nyka are with the Department of Microwave and Antenna Engineering, Faculty of Electronics, Telecommunications and Informatics, Gdansk University of Technology, 80-233 Gdańsk, Poland (e-mail: kamil.trzebiatowski@pg.edu.pl).

Lukasz Kulas is with the Department of Microwave and Antenna Engineering, Faculty of Electronics, Telecommunications and Informatics, Gdansk University of Technology, 80-233 Gdańsk, Poland, and also with the Digital Technologies Center, Gdansk University of Technology, 80-233 Gdańsk, Poland.

Digital Object Identifier 10.1109/LAWP.2024.3492276

© 2024 The Authors. This work is licensed under a Creative Commons Attribution 4.0 License. For more information, see https://creativecommons.org/licenses/by/4.0/

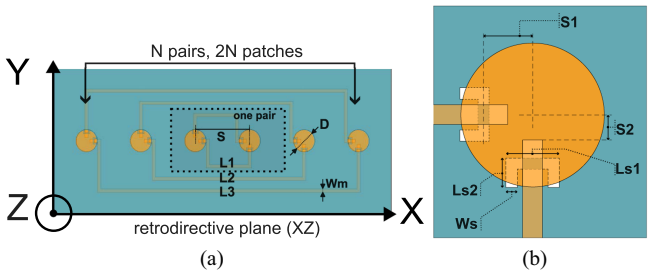

Fig. 1. Design and dimensions of: (a) base Van Atta arrays and (b) single radiating element.

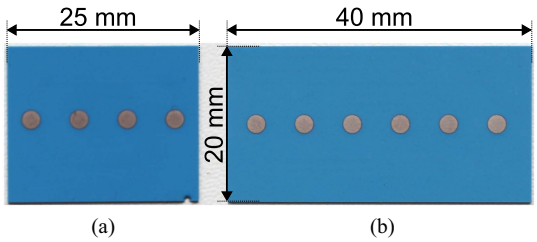

Fig. 2. Designed and manufactured Van Atta arrays: (a) N=2 and (b) N=3.

TABLE I
DIMENSIONS OF THE DESIGNED ARRAYS

Frequency (f_0)	24 GHz	**L_{s2}**	0.43 mm
λ_0	12.5 mm	**Ws**	0.15 mm
λ_D	4.627 mm	**Li, i = 1...N**	$L_0 + 3(i-1)\lambda_D$ L_0 = 11.76 mm
D	2.42 mm	**Wm**	0.36 mm
S	0.5 λ_0	**T1, T2**	0.2 mm, 0.2 mm
S1	0.39 mm	**Ls2**	0.43 mm
S2	0.84 mm	**Ws**	0.15 mm
Ls1	0.73 mm	***Li, i* = 1...N**	$L_0 + 3(i-1)\lambda_D$ L_0 = 11.76 mm
Size	N = 2: 20 mm × 25 mm		
	N = 3: 20 mm × 40 mm		

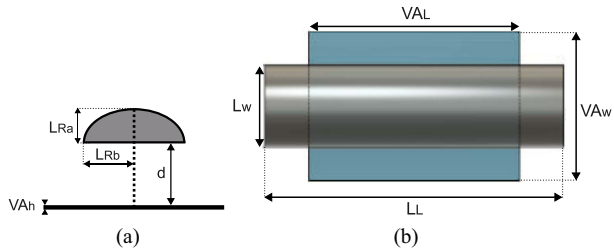

Fig. 3. Design and dimensions of the lenses. (a) YZ cross section. (b) Top view.

TABLE II
DIMENSIONS OF THE DESIGNED LENSES (IN MM)

Lens	VA_h	VA_L	VA_w	d	LR_a	L_w	LR_b	L_L
A	0.42	25.0	15.0	17.0	14.7	36.0	18.0	90.0
B	0.42	25.0	15.0	8.5	5.0	12.0	6.0	40.0
C	0.42	38.8	21.3	7.5	4.0	11.6	5.8	55.0

TABLE III
SIZES AND PHOTOGRAPHS OF THE DESIGNED ARRAYS WITH LENSES

Configuration	**f_0 = 24 GHz**	**Total size [mm × mm] × mm]**
Lens: A **Array: N = 2**	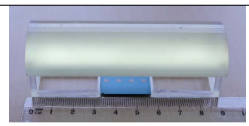	36 × 90 × 32.1
Lens: B **Array: N = 2**	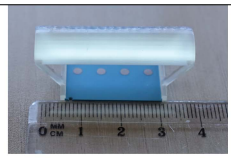	40 × 12 × 13.7
Lens: C **Array: N = 3**	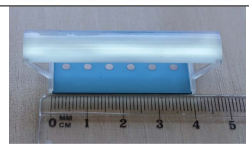	55 × 11.6 ×11.9

number of radiating elements in the array. However, this comes at the cost of enlarging and complicating the interconnecting network, particularly in the case of 2-D arrays. As a result, this approach faces diminishing returns due to the fact that the energy losses in the growing network prevent the RCS from increasing indefinitely. Moreover, practical implementations often require cross-polarized transmitting and receiving antennas to minimize interference from unwanted reflections (which are usually copolarized), further complicating the design of the network [3], [4], [13], [14], [15], [16], [17]. Other approaches to enhance the RCS without the need of employing such complex interconnecting networks involve high-gain individual antenna elements [12], [13], [14] or stacking multiple copies of the 1-D array in the direction perpendicular to the retrodirective axis [17], [18]. Both these methods lead to the narrowing of RCS beam in the perpendicular plane. The first technique also decreases the retrodirective angular range, as the beams of individual elements become more focused. In the second approach, the effect of beam narrowing in the perpendicular plane is much more pronounced, requiring precise alignment between the reader and the tag, thus becoming impractical for many applications.

To address these issues, we propose a new concept that increases the RCS of Van Atta arrays without extending the lengths of the interconnecting lines, thereby avoiding the diminishing returns associated with line losses. Our approach involves combining small low-RCS Van Atta arrays with gain-increasing 3-D printed dielectric lenses. To enhance the RCS of the tag while maintaining a wide angular range of retrodirective response in the main plane, lenses refracting in one plane are proposed. Although the lenses narrow the angular range in the perpendicular plane, this effect is less pronounced compared to stacking multiple closely spaced 1-D arrays.

The presented designs of Van Atta arrays are manufactured in low temperature co-fired ceramic (LTCC) technology, which enables the fabrication of multilayer structures that are durable and capable of withstanding harsh environmental conditions, such as high temperatures and humidity. This makes LTCC-based arrays (and chipless RFID tags) particularly suitable for industrial applications [20], [21].

In this letter, we present the design and fabrication of these 3-D printed lenses using stereolithography (SLA) technology

MOST WIEDZY Downloaded from mostwiedzy.pl

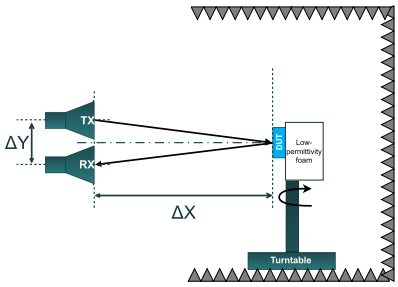

Fig. 4. Quasi-monostatic measurement setup.

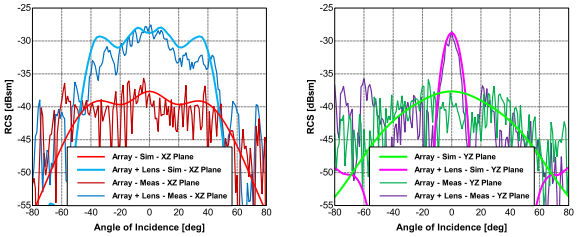

(a) (b)

Fig. 5. RCS patterns for configuration A. (a) *XZ* (retrodirective)-plane. (b) *YZ* (perpendicular)-plane.

with high-performance resin. We present the base Van Atta array in LTCC technology, discuss the integration with the 3-D printed lens, and compare the experimental results with numerical simulations. Our findings demonstrate substantial enhancement of the RCS levels, providing a viable path for creating high-RCS level Van Atta arrays to be used as a base for chipless RFID tags.

II. Van Atta Arrays Design

The base 1-D cross-polarized Van Atta array design with N pairs of microstrip patches [16], [18] is presented in Fig. 1(a). The design configuration and size can be modified by changing the N parameter. Two arrays having $N = 2$ and $N = 3$, respectively, were designed and manufactured for this research, as seen in Fig. 2.

The radiating elements are dual-polarized circular patches of diameter D, as shown in Fig. 1(b). The patches are fed by aperture-coupled microstrip lines through two orthogonal C-shaped slots [18], [19], characterized by the dimensions of L_{s1}, L_{s2}, and W_s. The slots are offset from the patch center by a distance S_1, while the feeding lines are positioned at a distance S_2 from the patch center. The aperture coupling technique reduces unwanted radiation from the interconnecting lines, as they are separated from the microstrip patches by a ground plane.

The microstrip lines of width W_m connect two orthogonal polarization ports in each antenna pair so the received and reradiated waves are of orthogonal polarization. The patches in the array are spaced by distance S equal to half of the free-space wavelength λ_0 at the design frequency f_0 (24 GHz in the presented designs). The lengths of the microstrip lines $L_i (i = 1 \ldots N)$ differ by a multiple of wavelength λ_D (in the microstrip line), so that all the patches are fed in-phase ($\pm n \cdot 360^\circ$). All the dimensions and their values are summarized in Table I. The presented Van Atta arrays are designed to be manufactured in the LTCC technology on GT951 ceramic substrate having

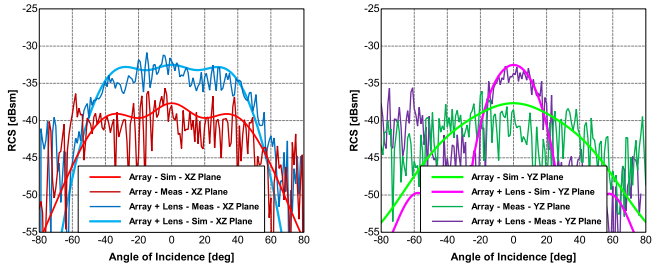

(a) (b)

Fig. 6. RCS patterns for configuration B. (a) *XZ* (retrodirective)-plane. (b) *YZ* (perpendicular)-plane.

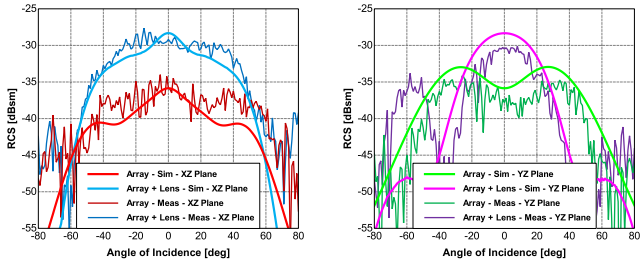

(a) (b)

Fig. 7. RCS patterns for configuration C. (a) *XZ* (retrodirective)-plane. (b) *YZ* (perpendicular)-plane.

TABLE IV
Summary of the Performance of the Presented Lenses

Measurements				
Configuration	Average RCS level [dBsm]		RCS angular range [°] Main / orthogonal direction	
	Without lens	With lens	Without lens	With lens
A	-41.4	-30.8	52 / 80	56 / 8
B	-41.4	-36.6	52 / 80	65 / 25
C	-37.2	-30.5	70 / 94	62 / 32
Simulations				
Configuration	Average RCS level [dBsm]		RCS angular range [°] Main / orthogonal direction	
	Without lens	With lens	Without lens	With lens
A	-39.2	-29.1	92 / 64	40 / 11
B	-39.2	-33.2	92 / 64	85 / 25
C	-37.2	-30.0	38 / 90	41 / 39

$\varepsilon_r = 7.3$ and $\tan\delta = 0.013$, in a process with two dielectric layers of thicknesses $T1$ and $T2$. The simulated maximum RCS values of the tags were: -37.7 dBsm for $N = 2$ and -35.8 dBsm for $N = 3$.

III. Lens Design

Three different lenses (A, B, and C) were designed to enhance the RCS of Van Atta arrays presented in Section II by increasing the effective gain of the radiators. Two lenses (A and B) of different sizes are proposed for the array with $N = 2$ to evaluate the influence of lenses' size on the RCS characteristics. Third lens (C) is proposed for the array with $N = 3$ to validate the presented RCS enhancement method for a different base array. The lenses are designed for 3-D printing using the SLA process and high-performance FormLabs High Temp resin with $\varepsilon_r = 2.66$ and $\tan\delta = 0.03$ [22].

MOST WIEDZY Downloaded from mostwiedzy.pl

TABLE V
COMPARISON OF THE RCS ENHANCEMENT TECHNIQUES

Ref.	Method	Area increase [ratio]	Thickness [mm]	RCS increase [dB]	Drawbacks
[14]	Increase of number of the antenna pairs	2.44	< 1	5	Limited by growing interconnecting network
[18]	Y-axis array multiplication	1.62	< 1	5	Significant reduction of angular range in perpendicular plane, high side-lobes
[17]		2	< 1	6	
[12]	Gain enhancement via sub-arrays	1.5*	< 1	8*	
Lens A	Dielectric lens	8.64	32.1	10.6	Reduction of angular range in perpendicular plane, low side-lobes
Lens B		1.6	13.7	4.8	
Lens C		1.42	11.9	6.7	

* estimated using the standard formula for RCS in the function of antenna gain [11].

The design goal was to focus the incident and retransmitted wave only in the *YZ* plane (perpendicular to the array's retrodirective plane) while preserving angular range (defined as the angle with an RCS decrease of 3 dB) in the *XZ* plane (the retrodirective plane) as wide as possible. To this end, the lenses were designed to refract the wave only on their curved surface in the *YZ* plane. The *YZ* cross section of the lenses is a half-ellipse with a semiminor axis of length L_{Ra} and a semimajor axis of length L_{Rb}. This shape was then extruded along the *X*-axis by a length of L_L, resulting in lenses uniform in one dimension. The lenses are positioned at a distance d from the array.

Cross sections in the *YZ* plane and top views of structures A, B, and C are presented in Fig. 3, while their photographs and dimensions are gathered in Tables II and III.

IV. EXPERIMENTAL VERIFICATION

The Van Atta arrays were manufactured by Fraunhofer Institute for Ceramic Technologies and Systems (IKTS) in a standard LTCC process with screen printing of the metallization layers [20]. The dielectric lenses were 3-D printed using SLA process and high-performance FormLabs High Temp resin [18]. The arrays with the lenses were tested in an anechoic chamber.

The RCS characteristics were measured in a quasi-monostatic setup, with cross-polarized transmitting and receiving antennas mounted on a rack and separated by $\Delta Y = 9$ cm, with the distance between the antennas' apertures and the device under test (DUT) $\Delta X = 100$ cm (see Fig. 4). The arrays were tested for incident wave angles in the range of $-80°$ to $80°$ by rotating them around their own axis using a turntable.

The simulated and measured RCS values in the function of angle of incidence are compared in Figs. 5–7. The measurements confirm the simulated values, although the presence of measurement errors is clearly visible. They are caused by a parallax angle between the measurement antennas, positioning errors, deviation of the DUT's plane from the vertical plane parallel to the range antennas' plane [18], and stochastic noise as single sweep measurements are presented.

The simulated energy losses in dielectric lenses are 0.7 dB (configuration A), 0.7 dB (B), and 0.2 dB (C). The lenses increase the RCS of the base microstrip Van Atta array by 10 dB (A), 5 dB (B), and 7 dB (C). The average RCS levels and angular ranges are summarized in Table IV. The RCS angular range is defined for a 3 dB drop relative to the maximum. For the measurements, it is calculated based on the best fit line due to noisy characteristics. Average RCS level in simulation is computed as the mean value within the RCS angular range. In measurements, it is calculated as the mean value within the RCS angular range taken from the simulation.

The *YZ*-plane patterns for arrays with lenses are notably narrower than the base arrays' patterns, as expected. The main *XZ*-plane patterns remain flat in a wide range of incidence angles. The results of the presented RCS enhancement technique are compared with the state-of-the-art methods in Table V.

V. CONCLUSION

In this letter, we presented a new way to increase the RCS level of small planar mmW Van Atta arrays by combining them with 3-D printed dielectric lenses. The presented arrays could be used as a base for frequency-encoded chipless RFID tags in at least two ways. The first option is to introduce bit-coding resonators in the interconnecting network [3]. The second option is to design a family of tags with different resonance frequencies and use them for object classification [15]. The employed lenses, depending on their size, can increase the RCS by up to 10 dB compared with the base array, directly increasing the read range, while preserving a wide angular range in the retrodirective plane, improving the angular detectability of the tag.

For a given Van Atta array, the lens can be easily interchanged to tailor the RCS pattern to the specific requirements of the desired application. Such an approach supports sustainability-oriented and circular economy-oriented designs, as it allows to fabricate only one variant of base Van Atta tags in large quantities, reducing the production costs. Another advantage of the presented technique is that it can be combined with any of the other methods compared in Table V to further enhance the RCS level. In addition, as LTCC tags are very durable, they can easily be repaired, modified, or reused by exchanging its lenses. The obvious disadvantage of the presented method is that the resulting tags become nonplanar and bulky, as the lenses are 3-D structures and are not placed directly on the array. The future work will be focused on the integration of lenses with the Van Atta arrays into a single LTCC structure and experimental evaluation of the presented design as a prototype of chipless RFID tag.

ACKNOWLEDGMENT

This letter reflects only the authors' views, and neither the European Union nor the granting authorities can be held responsible for them.

MOST WIEDZY Downloaded from mostwiedzy.pl

REFERENCES

[1] S. Tedjini, N. Karmakar, E. Perret, A. Vena, R. Koswatta, and R. E-Azim, "Hold the chips: Chipless technology, an alternative technique for RFID," *IEEE Microw. Mag.*, vol. 14, no. 5, pp. 56–65, Jul./Aug. 2013, doi: 10.1109/MMM.2013.2259393.

[2] P. Pursula et al., "Millimeter-wave identification—A new short-range radio system for low-power high data-rate applications," *IEEE Trans. Microw. Theory Techn.*, vol. 56, no. 10, pp. 2221–2228, Oct. 2008, doi: 10.1109/TMTT.2008.2004252.

[3] S. Preradovic and N. C. Karmakar, "Chipless RFID: Bar code of the future," *IEEE Microw. Mag.*, vol. 11, no. 7, pp. 87–97, Dec. 2010, doi: 10.1109/MMM.2010.938571.

[4] C. Herrojo, F. Paredes, J. Mata-Contreras, and F. Martín, "Chipless-RFID: A review and recent developments," *Sensors*, vol. 19, 2019, Art. no. 3385, doi: 10.3390/s19153385.

[5] H. Li, B. Wang, M. Wu, J. Zhu, and C. Zhou, "Design and analysis of chipless RFID tags based on retro-radiators," *IEEE Access*, vol. 7, pp. 148208–148217, 2019, doi: 10.1109/ACCESS.2019.2946614.

[6] C. Song et al., "Advances in wirelessly powered backscatter communications: From antenna/RF circuitry design to printed flexible electronics," *Proc. IEEE*, vol. 110, no. 1, pp. 171–192, Jan. 2022, doi: 10.1109/JPROC.2021.3125285.

[7] O. Rance, R. Siragusa, P. Lemaître-Auger, and E. Perret, "Toward RCS magnitude level coding for chipless RFID," *IEEE Trans. Microw. Theory Techn.*, vol. 64, no. 7, pp. 2315–2325, Jul. 2016, doi: 10.1109/TMTT.2016.2562625.

[8] N. Barbot, O. Rance, and E. Perret, "Classical RFID versus chipless RFID read range: Is linearity friend or a foe?," *IEEE Trans. Microw. Theory Techn.*, vol. 69, no. 9, pp. 4199–4208, Sep. 2021, doi: 10.1109/TMTT.2021.3077019.

[9] D. Girbau, A. Lázaro, and Á Ramos, "Time-coded chipless RFID tags: Design, characterization and application," in *Proc. 2012 IEEE Int. Conf. RFID-Tech. Appl.*, Nice, France, 2012, pp. 12–17, doi: 10.1109/RFID-TA.2012.6404497.

[10] L. C. Van Atta, "Electromagnetic reflector," U.S. Patent US2908002A, 1959.

[11] E. Sharp and M. Diab, "Van Atta reflector array," *IRE Trans. Antennas Propag.*, vol. AP-8, no. 4, pp. 436–438, Jul. 1960, doi: 10.1109/TAP.1960.1144877.

[12] J. G. D. Hester and M. M. Tentzeris, "Inkjet-printed flexible mm-Wave Van-Atta reflectarrays: A solution for ultralong-range dense multitag and multisensing chipless RFID implementations for IoT smart skins," *IEEE Trans. Microw. Theory Techn.*, vol. 64, no. 12, pp. 4763–4773, Dec. 2016, doi: 10.1109/TMTT.2016.2623790.

[13] A. Vena, E. Perret, and S. Tedjni, "A depolarizing chipless RFID tag for robust detection and its FCC compliant UWB reading system," *IEEE Trans. Microw. Theory Techn.*, vol. 61, no. 8, pp. 2982–2994, Aug. 2013, doi: 10.1109/TMTT.2013.2267748.

[14] K. Trzebiatowski, M. Rzymowski, L. Kulas, and K. Nyka, "60 GHz microstrip Van Atta arrays for millimeter wave identification and localization," in *Proc. 23rd Int. Microw. Radar Conf.*, Warsaw, Poland, 2020, pp. 132–135, doi: 10.23919/MIKON48703.2020.9253855.

[15] K. Trzebiatowski, M. Rzymowski, L. Kulas, and K. Nyka, "Simple millimeter wave identification system based on 60 GHz Van Atta arrays," *Sensors*, vol. 22, 2022, Art. no. 9809, doi: 10.3390/s22249809.

[16] A. Di Carlofelice, E. Di Giampaolo, and P. Tognolatti, "A Van-Atta UWB cross-polar chipless tag to be used as a sensor," in *Proc. 2023 Photon. Electromagn. Res. Symp.*, Prague, Czech Republic, 2023, pp. 698–702, doi: 10.1109/PIERS59004.2023.10221272.

[17] X.-F. Li, Y.-L. Ban, Q. Sun, Y.-X. Che, J. Hu, and Z. Nie, "A compact dual-band Van Atta array based on the single-port single-band/dual-band antennas," *IEEE Antennas Wireless Propag. Lett.*, vol. 22, no. 4, pp. 888–892, Apr. 2023, doi: 10.1109/LAWP.2022.3227577.

[18] K. Trzebiatowski, M. Ihle, B. Sikorski, L. Kulas, and K. Nyka, "Millimeter wave retrodirective Van Atta arrays in LTCC technology," in *Proc. 18th Eur. Conf. Antennas Propag.*, Glasgow, U.K., 2024, pp. 1–5, doi: 10.23919/EuCAP60739.2024.10501427.

[19] K. Trzebiatowski, W. Kalista, M. Rzymowski, L. Kulas, and K. Nyka, "Multibeam antenna for Ka-band CubeSat connectivity using 3-D printed lens and antenna array," *IEEE Antennas Wireless Propag. Lett.*, vol. 21, no. 11, pp. 2244–2248, Nov. 2022, doi: 10.1109/LAWP.2022.3189073.

[20] M. Ihle, S. Ziesche, C. Zech, and B. Baumann, "Compact LTCC packaging and printing technologies for sub-THz modules," in *Proc. 7th Electron. System-Integr. Tech. Conf.*, Dresden, Germany, 2018, pp. 1–4, doi: 10.1109/ESTC.2018.8546400.

[21] D. Nowak and A. Dziedzic, "LTCC package for high temperature applications," *Microelectron. Rel.*, vol. 51, no. 7, pp. 1241–1244, 2011, doi: 10.1016/j.microrel.2011.02.018.

[22] G. B. Wu, Y. S. Zeng, K. F. Chan, S. W. Qu, and C. H. Chan, "3-D printed terahertz lens with circularly polarized focused near field," in *Proc. 13th Eur. Conf. Antennas Propag.*, Krakow, Poland, 2019, pp. 1–4.

MOST WIEDZY Downloaded from mostwiedzy.pl